Original paper

Clean Prod Processes 3 (2001) 92–103
DOI 10.1007/s100980100112

# Design of multi-phase and catalytic chemical reactors: a simulation tool for pollution prevention

**Jack R. Hopper, Jamal M. Saleh, Ralph Pike**



**Abstract** A comprehensive chemical reactor analysis tool was required to complete a project to develop an advanced on-line process optimization analysis system for pollution prevention. The advanced process analysis system integrates programs (reactors, on-line optimization, pinch analysis, and process flow-sheeting) to analyze and modify chemical processes for waste minimization. The reactor analysis program is to be used to evaluate and analyze multi-phase and catalytic reactors to suggest to the plant and process engineers the best reactor type and operating conditions. A multi-phase catalytic reactor design and analysis tool, ReaCat, has been developed. ReaCat incorporates models to design the following reactor types: plug flow, CSTR, batch, catalytic fixed-bed, catalytic fluidized-bed, gas–liquid stirred tank, trickle-bed, three-phase fixed bubble-bed, bubble slurry column, CSTR slurry, and three-phase fluidized-bed. This paper gives a summary of the multi-phase and catalytic reactors: classifications, theory and design models, numerical methods, and solution algorithms. A description of the reactor analysis tool including comparison cases with experimental data is presented.

## List of symbols

| | |
|---|---|
| $A$ | Heat transfer area ($m^2$) |
| $C_{G,i}$ | Gas bulk concentration of component $i$ (mol/l) |
| $C^{i}_{G,i}$ | Inlet bulk gas concentration of component $i$ (mol/l) |
| $C^{o}_{G,i}$ | Outlet bulk gas concentration of component $i$ (mol/l) |
| $C_{L,i}$ | Liquid bulk concentration of component $i$ (mol/l) |
| $C^{i}_{L,i}$ | Inlet bulk liquid concentration of component $i$ (mol/l) |
| $C^{o}_{L,i}$ | Outlet bulk liquid concentration of component $i$ (mol/l) |
| $C_{S,i}$ | Concentration of component $i$ at catalyst surface (mol/l) |
| $C_{pg}$ | Specific heat capacity of gas [(BTU/°F lb.) cal/Kg] |
| $C_{pL}$ | Specific heat capacity of liquid [(BTU/°F lb.) cal/K g] |
| $D_A$ | Bulk diffusivity ($cm^2/s$) |
| $D_{L,i}$ | Liquid-phase axial dispersion coefficient ($cm^2/s$) |
| $E$ | Energy of activation (kJ/mol) |
| $F_{gas}$ | Flow rate of gas ($m^3/s$) |
| $F^{i}_{i}$ | Inlet flow rate for component $i$ |
| $\Delta H_{ri}$ | Heat of reaction of the component $i$ (kJ/mol) |
| $H_i$ | Henry's constant for component $i$ |
| $K$ | First-order reaction constant |
| $K_{BC}$ | Gas-phase (bubble-phase) mass transfer coefficient (1/s) |
| $K_{CE}$ | Intermediate (cloud-wake) phase mass transfer coefficient (1/s) |
| $K_c a_c$ | Liquid–solid mass transfer coefficient (1/s) |
| $(K_L a_g)_i$ | Gas–liquid mass transfer coefficient for component $i$ (1/s) |
| $(K_c a_c)_i$ | Liquid–solid mass transfer coefficient for component $i$ (1/s) |
| $K_g a_L$ | Gas-phase mass transfer coefficient (1/s) |
| $K_L a_L$ | Liquid-phase mass transfer coefficient (1/s) |
| $k_s$ | First-order reaction constant |
| $N_s$ | Number of species in mixture |
| $P^{i}_{i}$ | Inlet bulk gas partial pressure of component $i$ [(psi) bar] |
| $P^{o}_{i}$ | Outlet bulk gas partial pressure of component $i$ [(psi) bar] |
| $Q_G$ | Gas volumetric flow rate ($cm^3/s$) |
| $Q_L$ | Liquid volumetric flow rate ($cm^3/s$) |
| $Q_{Gmax}$ | Maximum gas flow rate ($cm^3/s$) |
| $R$ | Gas constant (l atm/mol K) |
| $(-r_i)$ | Net rate of disappearance of component $i$ |
| $t$ | Time (s) |
| $T_i$ | Inlet temperature [(°F) K] |
| $T_o$ | Outlet temperature [(°F) K] |
| $T_a$ | Ambient temperature [(°F) K] |
| $U$ | Overall heat transfer coefficient [BTU/h $ft^2$ °F (cal/s $cm^2$ K)] |
| $U_G$ | Gas superficial velocity (cm/s) |
| $U_b$ | Bulk gas-phase velocity (cm/s) |
| $U_L$ | Liquid superficial velocity (cm/s) |
| $V_R$ | Reactor volume ($m^3$) |
| $V_T$ | Volume of reservoir ($m^3$) |

Received: 20 January 2000 / Accepted: 2 April 2001
Published online: 10 July 2001


J.R. Hopper (✉), J.M. Saleh
Lamar University, Chemical Engineering Department,
P.O. Box 10053, Beaumont, TX 77710, USA
E-mail: hopperjr@hal.lamar.edu

R. Pike
Louisiana State University, Baton Rouge, Louisiana, USA

Support from the Gulf Coast Hazardous Substance Research Center and the Environmental Protection Agency is gratefully acknowledged

$z$ Axial position (cm)
$\rho_L$ Density of liquid (g/cm$^3$)
$\tau$ Gas-space time ($V_R/Q_G$) (s)

## Introduction

To perform an advanced process system analysis, which is used to evaluate chemical and refinery processes for waste minimization (Telang 1996, Pike et al. 1998), an advanced chemical reactor tool is essential. The reactor design tool is to be used to evaluate and analyze the various types of industrial multi-phase and catalytic reactors. In an effective and time saving manner, plant and process engineers need a reactor design tool to analyze and study the effect of operating conditions on the pollution index. For this purpose, ReaCat, a multi-phase catalytic reactor analysis simulation tool, has been developed with the following features:

1. User-friendly input/output interface
2. Graphical and tabular data output
3. Reactor models included
   - i Homogeneous reactors (plug flow, CSTR, batch)
   - ii Heterogeneous reactors
   - I Catalytic gas fixed-bed
   - II Catalytic liquid fixed-bed
   - III Catalytic gas fluidized-bed
   - IV Catalytic liquid fluidized-bed
   - V Gas–liquid continuous stirred tank
   - VI Three-phase trickle-bed
   - VII Three-phase bubble fixed-bed
   - VIII Three-phase catalytic gas–liquid slurry stirred tank
   - XI Three-phase catalytic gas–liquid slurry bubble-bed
   - X Three-phase catalytic gas–liquid fluidized-bed
4. Power-law reaction rate or the Langmuir–Hinshelwood model to account for the catalytic adsorption effects
5. Equipped with correlation to estimate the external mass transfer effects (gas–liquid, and liquid–solid), and dispersion coefficients
6. Estimation of the catalytic effectiveness factor to account for the intra-particle resistance
7. Isothermal and non-isothermal/non-adiabatic conditions
8. Multi-reaction systems with up to 30 reactions and 36 components
9. Prediction of reactor hydrodynamics such as pressure drop, power consumption, catalyst-wetting factor, and flow regimes.

## Multi-phase and catalytic reactor, definitions and classifications

In industrial chemical processes, multi-phase reactors have a wide range of applications such as oxidation, hydrogenation, hydro-desulfurization, and the Fischer–Tropsch synthesis. Table 1 lists the definition for the different reactor types included in this study. Multi-phase reactors are defined as reactors with at least two distinct phases in contact. Reactors, in general, may be classified based on the number of phase coexistence into the following category:

i) Homogeneous: one phase such as gas or liquid exists in the reactor. The hydrodynamic flow characteristic of the mixture determines the reactor type such as plug, CSTR, or batch.
ii) Heterogeneous: two distinct phases of reactants (or catalyst) coexist. This category may be classified into the following subcategories:
   a Catalytic reactors: gas or liquid phase (or both) is in contact with a catalyst (mainly solid, but could be another liquid phase). Examples of this category include the catalytic packed-bed (catalytic gas reaction) and the three-phase trickle-bed (catalytic gas–liquid reaction).
   b Non-catalytic reactors: gas–liquid or liquid–liquid reactions are carried in a variety of contact vessels such as the gas–liquid continuously stirred tank reactor.

Each reactor type exhibits certain characteristics and advantages that may make it the best candidate for a specific reaction; the power of a simulation tool becomes very clear for such an analysis. For a complete discussion on examples, classification, definitions, and advantages or disadvantages of multi-phase and catalytic industrial reactors, the reader is referred to Ostergaard (1974), Shah (1979), Tarhan (1979), Ramachandran and Chaudhari (1983), Tsutsumi et al. (1987), and Saleh (1994).



**Table 1.** Definitions of reactors

| | |
|---|---|
| Catalytic packed-bed | Gas or liquid reactants flow over a fixed-bed of catalysts |
| Catalytic fluidized-bed | The up-flow gas or liquid phase suspends the fine catalyst particles |
| CSTR gas–liquid | Liquid and gas phases are mechanically agitated |
| Bubble gas–liquid bed | Liquid phase is agitated by the bubble rise of the gas phase. Liquid phase is continuous |
| Trickle-bed | Concurrent down-flow of gas and liquid over a fixed-bed of catalyst. Liquid trickles down, while gas phase is continuous |
| Bubble fixed-bed | Concurrent up-flow of gas and liquid. Catalyst bed is completely immersed in a continuous liquid flow while gas rises as bubbles |
| CSTR slurry | Mechanically agitated gas–liquid catalyst reactor. The Fine catalyst particles are suspended in the liquid phase by means of agitation. (Batch liquid phase may also be used) |
| Bubble slurry column | Liquid is agitated by means of the dispersed gas bubbles. Gas bubble provides the momentum to suspend the catalyst particles |
| Three-phase fluidized-bed | Catalyst particles are fluidized by an upward liquid flow while gas phase rises in a dispersed bubble regime |

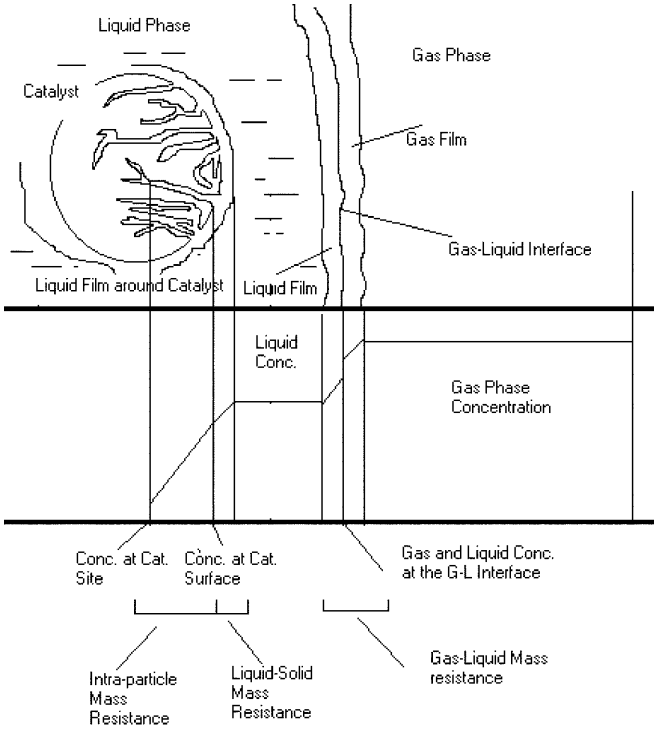


**Fig. 1.** Gas–liquid–solid contact in three-phase reactors

## Design models

Design of multi-phase and catalytic reactors is more complex than that of homogeneous reactors due to the following: the coexistence of more than one phase introduces the mass transfer resistance (Fig 1), the intra-particle diffusion, adsorption effects, and the flow regimes, which may be different for each phase. The details of the mathematical model, assumptions, and solution algorithm for each of the reactor types are listed in Saleh (1994), Hedge (1999), and Waghchoure (1999). Tables 2, 3, 4, 5, 6, and 7 show the design model, assumptions, and solution algorithms for the three-phase trickle-bed, three-phase catalytic slurry CSTR, and gas–liquid (non-catalytic) agitated tank, catalytic liquid fluidized-bed, catalytic gas fluidized-bed, and catalytic fixed-bed, respectively. The trickle-bed model (Table 2) is applicable to three-phase fixed-bed, three-phase fluidized-bed, and three-phase bubble slurry-bed as well. A complete list of correlations implemented in the ReaCat program to predict the mass transfer and hydrodynamic parameters are listed in Saleh (1994), Hedge (1999), and Waghchoure (1999). The selection of these correlations is based on the recommendation, found in literature review, of other authorities in this area. For examples, the correlation implemented for the three-phase reactors are those recommended by Ramachandran and Chaudhari (1983). Since most of the correlations were developed for laboratory and pilot reactors, program users are allowed to skip correlation when experimental data are available. Tables 8 and 9 give a summary of the correlations used in the program. For catalytic reactors, intra-particle diffusion is accounted for by multiplying the intrinsic reaction rate by the catalytic effectiveness factor. The procedure to estimate the catalytic effectiveness factor is listed in Table 10. Procedures to warn the user of conditions that violate the model assumptions are also included. For example, when the catalyst-wetting factor is not unity or when a flow regime

**Table 2.** Three-phase gas–liquid catalytic reactors design model (trickle-bed, fixed-up-flow bubble-bed, bubble slurry bed, three-phase fluidized-bed)

| | | |
|---|---|---|
| Non-volatile liquid-phase mass balance | $D_{L,i}\frac{d^2CL,i}{dz^2} - U_L\frac{dCL,i}{dz} - (K_c a_c)_i\left(C_{L,i} - C_{S,i}\right) = 0.0$ | (1) |
| Volatile liquid-phase mass balance | $D_{L,i}\frac{d^2CL,i}{dz^2} - U_L\frac{dCL,i}{dz} + \left(K_L a_g\right)_i\left(\frac{CG,i}{Hi} - C_{L,i}\right) - (K_c a_c)_i\left(C_{L,i} - C_{S,i}\right) = 0.0$ | (2) |
| Boundary conditions | At $z = 0 \quad -D_{L,i}\frac{dCL,i}{dz} = U_L\left(C_{L,i} - C^{i}_{L,i}\right)$ | |
| | At $z = L \quad \frac{dCL,i}{dz} = 0$ | |
| Gas-phase mass balance | $-U_g\frac{dCg,i}{dz} - \left(K_L a_g\right)i\left(\frac{CG,i}{Hi} - C_{L,i}\right) = 0.0$ | (3) |
| Component mass balance around the catalyst | $(K_c a_c)_i\left(C_{L,i} - C_{S,i}\right) = (-r_i)$ | (4) |

Model assumptions

1. Complete radial mixing
2. Axial back mixing is accounted for by the dispersion parameter
3. Gas and liquid concentration and temperature profiles are function of reactor length only
4. Complete catalyst-wetting factor and uniform catalyst concentration and activity
5. The catalytic effectiveness factor accounts for the intra-particle diffusion resistance

Solution algorithm

1. Equations 1–4 are developed for each component in mixture
2. At the inlet of reactor, $z$=0, the nonlinear algebraic system of Eq. 4 is solved the concentration at the catalyst surface by the Newton–Raphson numerical method
3. When plug flow model is assumed, Eqs. 2, 3, and 4 are integrated using the previously calculated surface concentration. For the dispersion model, the shooting method is applied
4. Steps 1–3 are repeated for the entire reactor length

developed is other than the assumed, a warning message will be displayed at the end of the calculation. Each of the mathematical models has been tested versus other published experimental or simulation work. Table 11 lists some comparison examples; for more examples the reader may refer to Saleh (1994).

## Program description

A user-friendly input/output program has been developed to solve and analyze the different reactor types. Figures 2, 3, and 4 show a few of input screens. A complete user manual may be requested from the authors. Results may be viewed in graphical or tabular format. The user can view conversion, concentration, temperature, and pressure, which may be displayed as a function of reactor length, volume, catalyst weight, or reaction time (Fig 5). Another version of ReaCat was built to allow simple flowsheeting capability, such as connecting reactors in series or parallel, generic mixing and splitting of streams, and generic heat transfer equipment (Fig 6).

## Example 1, sulfuric acid production by contact process

The production of sulfuric acid by the contact process is a three-step process that produces sulfuric acid and steam from air, molten sulfur, and water. The process consists of three sections: (1) the feed preparation section; (2) the reactor section; (3) the absorber section. In the feed preparation section, molten sulfur feed is combusted with dry air in the sulfur burner to produce $SO_2$. The second section is the reactor or converter section. Gases from the feed section, sulfur dioxide and air, enter at (787 °F) 419.4 °C and (19.4 Psia) 133,759.12 Pa. Sulfur dioxide and



**Table 3.** Three-phase gas–liquid catalytic reactors design model (CSTR slurry)

| | | |
|---|---|---|
| Non-volatile component liquid-phase mass balance | $Q_{\mathrm{L}}\left(C^{\mathrm{i}}_{\mathrm{L},i} - C^{\mathrm{o}}_{\mathrm{L},i}\right) - V_{\mathrm{R}}(K_{\mathrm{c}}a_{\mathrm{c}})_i\left(C^{\mathrm{o}}_{\mathrm{L},i} - C_{\mathrm{S},i}\right) = 0.0$ | (1) |
| Non-volatile component liquid-phase mass balance | $Q_{\mathrm{L}}\left(C^{\mathrm{i}}_{\mathrm{L},i} - C^{\mathrm{o}}_{\mathrm{L},i}\right) + V_{\mathrm{R}}\left(K_{\mathrm{L}}a_{\mathrm{g}}\right)_i\left(\frac{C^{\mathrm{o}}\mathrm{G},i}{Hi} - C^{\mathrm{o}}_{\mathrm{L},i}\right) - V_{\mathrm{R}}(K_{\mathrm{c}}a_{\mathrm{c}})_i\left(C^{\mathrm{o}}_{\mathrm{L},i} - C_{\mathrm{S},i}\right) = 0.0$ | (2) |
| Gas-phase mass balance | $Q_{\mathrm{G}}\left(C^{\mathrm{i}}_{\mathrm{G},i} - C^{\mathrm{o}}_{\mathrm{G},i}\right) - V_{\mathrm{R}}\left(K_{\mathrm{L}}a_{\mathrm{g}}\right)_i\left(\frac{C^{\mathrm{o}}\mathrm{G},i}{Hi} - C^{\mathrm{o}}_{\mathrm{L},i}\right) = 0.0$ | (3) |
| Component mass balance around the catalyst | $V_{\mathrm{R}}(K_{\mathrm{c}}a_{\mathrm{c}})_i\left(C^{\mathrm{o}}_{\mathrm{L},i} - C_{\mathrm{S},i}\right) = V_{\mathrm{R}}(-r_i)$ | (4) |

Model assumption
1. Gas and liquid phases are well agitated
2. Uniform concentration and temperature within each phase in the entire reactor volume
3. Complete and homogeneous catalyst suspension
4. Continuous flow

Solution algorithm
1. Equations 1–4 are developed for each component in mixture
2. An initial guess for the surface concentration is assumed
3. For a given reactor volume, the system of nonlinear algebraic equations is solved iteratively by the Newton–Raphson method to find the exit conditions

**Table 4.** Gas–liquid agitated tank, design model

| | | |
|---|---|---|
| Gas-phase component mass balance | $(Q_{\mathrm{G}}/RT)\left(P^{\mathrm{i}}i - P^{\mathrm{o}}i\right) + V_{\mathrm{R}}EK_{\mathrm{G}}a_{\mathrm{L}}\left(P^{\mathrm{o}}i/Hi - C^{\mathrm{o}}_{Li}\right) = 0$ | (1) |
| or | $F_{\mathrm{gas}}/P_{\mathrm{T}}\left(P^{\mathrm{i}}i - P^{\mathrm{o}}i\right) - V_{\mathrm{R}}EK_{\mathrm{G}}a_{\mathrm{L}}\left(P^{\mathrm{o}}_i/Hi - C^{\mathrm{o}}_{\mathrm{L}i}\right) = 0$ | |
| Liquid-phase volatile-component mass balance | $Q_{\mathrm{L}}\left(C^{\mathrm{i}}_{\mathrm{L}i} - C^{\mathrm{o}}_{\mathrm{L}i}\right) + V_{\mathrm{R}}EK_{\mathrm{L}}a_{\mathrm{L}}\left(P^{\mathrm{o}}i/Hi - C^{\mathrm{o}}_{\mathrm{L}i}\right) + r_iV_{\mathrm{R}} = 0$ | (2) |
| Liquid-phase non-volatile-component mass balance | $Q_{\mathrm{L}}\left(C^{\mathrm{i}}_{\mathrm{L}i} - C^{\mathrm{o}}_{\mathrm{L}i}\right) + r_iV_{\mathrm{R}} = 0$ | (3) |
| Energy balance | $\Sigma F^{\mathrm{i}}i\left[\alpha_i(T\mathrm{i} - T\mathrm{o}) + \beta_i/2\left(T\mathrm{i}^2 - T\mathrm{o}^2\right) + \gamma_i/3\left(T\mathrm{i}^3 - T\mathrm{o}^3\right)\right] - \left[V_{\mathrm{R}}\Sigma(\Delta H_{\mathrm{r}i}r_i)\right] + UA(T\mathrm{a} - T\mathrm{o}) = 0$ | (4) |

Model assumption
1. Steady state
2. Both phases are assumed to be perfectly macro-mixed
3. Uniform gas and liquid temperature

Solution algorithm
1. Provide an initial guess for the design variables: gas and liquid concentrations and temperature
2. Estimate the hydrodynamic parameters: mass transfer coefficients, power consumption, and minimum gas flow rate
3. Equations 1–4 are developed for each component in mixture
4. The system of non-linear algebraic equation is solved simultaneously by the Newton–Raphson method

oxygen from air react with each other to produce $SO_3$ and heat since this is an exothermic reaction. $SO_3$ from the reactor section is passed to the absorber section where it reacts with water to form sulfuric acid. In the actual process plant, four converters are used to obtain maximum possible conversion with intermediate removal of heat and

**Table 5.** Catalytic liquid fluidized-bed reactors, design model

Liquid-phase component balance

Plug flow

$$-U_{\mathrm{L}}\frac{\mathrm{d}C_{i\mathrm{L}}}{\mathrm{d}Z}=K_{\mathrm{L}}(C_{i\mathrm{L}}-C_{i\mathrm{S}}) \quad (1)$$

Dispersion

$$D_{\mathrm{L}a}\frac{\mathrm{d}^2C_{i\mathrm{L}}}{\mathrm{d}Z^2}-U_{\mathrm{L}}\frac{\mathrm{d}C_{i\mathrm{L}}}{\mathrm{d}Z}=K_{\mathrm{L}}(C_{i\mathrm{L}}-C_{i\mathrm{S}}) \quad (2)$$

Catalyst (emulsion) phase

$$K_{\mathrm{L}}(C_{i\mathrm{L}}-C_{i\mathrm{S}})=(R)_{i\mathrm{CatalystPhase}} \quad (3)$$

Energy balance

$$\rho_{\mathrm{L}}U_{\mathrm{L}}C_{\mathrm{pL}}\frac{\mathrm{d}T}{\mathrm{d}Z}=\sum_{j=1}^{NR}Rj\Delta Hr_j+Ua(T_{\mathrm{ambient}}-T_{\mathrm{Reactor}}) \quad (4)$$

Assumptions

1. The reaction in the liquid phase is assumed negligible
2. By neglecting internal convection effects, the catalyst and the liquid are assumed to be at the same temperature based on the extremely small particle sizes. (in μm)
3. Steady state

Solution algorithm

1. Estimate the required parameters. ($U_{\mathrm{L}}$, $K_{\mathrm{L}}$, expanded length of bed)
2. Catalyst surface concentrations (Eq. 3) are converged using the Newton–Raphson method with the Gauss–Jordan elimination method. As a starting guess, catalyst phase concentrations are assumed to be equal to concentrations in liquid phase
3. Liquid concentrations (Eq. 1 or 2) for the next interval are calculated depending on type of the flow selected. (4th order Runge–Kutta for plug flow, finite difference for the dispersion model)

**Table 6.** Catalytic gas-fluidized-bed reactor, design model

Design equations

*Bulk gas phase (bubble phase)*

Plug flow

$$-U_{\mathrm{b}}\frac{\mathrm{d}C_{i\mathrm{b}}}{\mathrm{d}Z}=K_{\mathrm{BC}}(C_{i\mathrm{b}}-C_{i\mathrm{c}}) \quad (1)$$

With axial dispersion

$$D_{\mathrm{ga}}\frac{\mathrm{d}^2C_{i\mathrm{b}}}{\mathrm{d}Z^2}-U_{\mathrm{b}}\frac{\mathrm{d}C_{i\mathrm{b}}}{\mathrm{d}Z}=K_{\mathrm{BC}}(C_{i\mathrm{b}}-C_{i\mathrm{c}}) \quad (2)$$

*Intermediate (cloud-wake) phase*

$$K_{\mathrm{BC}}(C_{i\mathrm{b}}-C_{i\mathrm{c}})=\chi_{\mathrm{c}}(R)_{i\mathrm{CloudPhase}}+K_{\mathrm{CE}}(C_{i\mathrm{c}}-C_{i\mathrm{e}}) \quad (3)$$

*Catalyst (emulsion) phase*

$$K_{\mathrm{CE}}(C_{i\mathrm{c}}-C_{i\mathrm{e}})=\chi_{\mathrm{e}}(R)_{i\mathrm{EmulsionPhase}} \quad (4)$$

*Energy balance*

$$\rho_{\mathrm{g}}U_{\mathrm{b}}C_{\mathrm{pg}}\frac{\mathrm{d}T}{\mathrm{d}Z}=\sum_{j=1}^{NR}Rj\Delta Hr_j+Ua(T_{\mathrm{ambient}}-T_{\mathrm{Reactor}}) \quad (5)$$

Assumptions

1. Three phases present in a gas fluidized-bed reactor. Bulk gas phase is known as bubble phase. Intermediate phase contains both gas and the solids. Catalyst (emulsion) phase has solids in higher concentration
2. The gas bubbles formed are assumed to be spherical in nature
3. Mass transfer is believed to be happening in all three phases
4. The reaction occurring in bulk gas (bubble) phase is not significant and hence is neglected
5. Steady state

Solution algorithm

1. Estimate the required parameters using correlations. ($D_{\mathrm{b}}$, $U_{\mathrm{b}}$ $\gamma_{\mathrm{c}}$, $\gamma_{\mathrm{e}}$, $K_{\mathrm{BC}}$, $K_{\mathrm{CE}}$)
2. Intermediate and solid surface concentrations (Eqs. 3 and 4) are converged using the Newton–Raphson method with the Gauss–Jordan elimination method
3. Bulk gas concentrations (Eqs. 1 or 2) for the next interval are calculated depending on type of flow selected. (4th order Runge–Kutta for plug flow, finite difference for the dispersion model)
4. For non-isothermal cases, the temperature for the next interval is calculated by Eq. 5 and used to find reaction rates for the next length interval
5. Steps 3 and 4 are repeated over the total reactor length

the product, $SO_3$. The removal increases the equilibrium conversion. The reaction takes place on a vanadium pentoxide catalyst. Two types of this catalyst LP-110 and LP-120 are used in these reactors. The reaction is:

$$SO_2 + (1/2)O_2 \rightarrow SO_3$$

The kinetic model for this reaction was given by Harris and Norman (1972). The reaction rate is predicted by the following expression:

$$r_{SO2} = \frac{P'_{SO2}P'^{1/2}_{O2}}{\left(A + BP'^{1/2}_{1O2} + CP'_{SO2} + DP_{SO3}\right)^2}\left[1 - \frac{P_{SO3}}{K_P P_{SO2}P^{1/2}_{O2}}\right]$$

where

**Table 7.** Catalytic fixed-bed, design model

| | | |
|---|---|---|
| Mass balance around the catalyst | $(k_c a_c)_i (C_G - C_S)i = \eta(-R\text{net})_i$ | (1) |
| Gas-phase component mass balance (plug flow model) | $-U_G \frac{dCGi}{dz} - (k_c a_c)_i (C_G - C_S)i = 0.0$ | (2) |
| Gas-phase component mass balance (dispersion model) | $D_G i \frac{d^2 CGi}{d^2 z} - U_G \frac{dCGi}{dz} - (k_c a_c)_i (C_G - C_S)i = 0.0$ | (3) |
| Energy model | $U_G \rho_G Cp_G \frac{dT}{dz} = \sum (Rj\Delta HRj) + UA(T - Ta)$ | (4) |

Model assumptions
1. Complete radial mixing
2. Dispersion coefficient is used to account for the axial back mixing
3. Effectiveness factor accounts for the intra-particle resistance
4. Steady state

Solution algorithm
1. At the reactor inlet, develop Eq. 1 for each component in the mixture
2. Solve the system of non-linear algebraic equations for the concentration at the catalyst surface, $C_s$. This is an iterative procedure as follow: Guess $C_s$, solve for the effectiveness factor, evaluate the net intrinsic reaction rate for each component, then using the Newton–Raphson method to solve the system of Eqs. 1, new values for $C_s$ are estimated. The process is repeated till no further change in $C_s$ is occurring
3. Develop Eqs. 2 or 3 (depending on the model choice, plug or dispersion) for each component in mixture; solve for the next increment in reactor length using the 4th order Runge–Kutta method or finite difference
4. Repeat the above steps for the next reactor length increment

**Table 8.** Correlation used for the three-phase catalytic reactors

| Correlation | Trickle-bed | Fixed up-flow | CSTR slurry | Bubble slurry | Three-phase fluidized |
|---|---|---|---|---|---|
| Pressure drop | Larkins et al. (1961)<br>Ellman et al. (1988) | Turpin and Hintington (1967) | – | – | – |
| L and G holdup<1 | Sato et al. (1973)<br>Ellman et al. (1990) | Fukushima and Kusaka (1979)<br>Achwal and Stepanek (1976) | Calderbank (1958)<br>Yung et al. (1979) | Yamashita and Aeon (1975)<br>Maselker (1970) | Kim et al. (1975) |
| G–L mass transfer coefficient | Ellman et al. (1988)<br>Sato et al. (1973) | Reiss (1967) | Bern et al. (1976) | Akita and Yoshida (1974) | Dhanuka and Stepanek (1980)<br>Dakshinamurthy et al. (1974) |
| L–S mass transfer coefficient | Van Krevelen and Krekels (1948)<br>Dharwadker and Sylvester (1977) | Specchia et al. (1978) | Sano et al. (1974) | Kobayashi and Saito (1965) | Lee et al. (1974) |
| L dispersion coefficient | Michell and Furzer (1972) | Stiegel and Shah (1977) | – | Deckwer et al. (1974) | El-Temtamy et al. (1979) |
| G dispersion coefficient | Hochman and Effron (1969) | – | – | Mangartz and Pilhofer (1981) | – |
| Wall heat transfer coefficient | Specchia and Baldi (1979) | – | – | Fair (1967) | – |
| Power consumption | – | – | Luong and Volesky (1979)<br>Michel and Miller (1962) | – | – |

$P_{SO2}$, $P_{O2}$, $P_{SO3}$ are interfacial partial pressures of $SO_2$, $O_2$, and $SO_3$ (atm)
$K_P$ is the thermodynamic equilibrium constant ($atm^{-1/2}$)
Constants $A$, $B$, $C$, and $D$ are function of temperature $T$
$P'$ denotes interfacial partial pressures of $SO_2$ and $O_2$ zero conversion under total pressure at the point or reactor (atm)

For catalyst type LP-110

$$A = e^{-6.8+4960/T}, B = 0, C = e^{10.32-7350/T}, D = e^{-7.38+6370/T}$$



For catalyst type LP-120

$$A = e^{-5.89+4060/T}, B = 0, C = e^{6.45-4610/T}, D = e^{-8.59+7020/T}$$

For the heat of reaction, an empirical formula is used, which was also derived by Harris and Norman (1972):

$$\Delta H_{\text{reaction}} = 1.827(-24097 - 0.26T + 1.69 \times 10^{-3}T^2 + 1.5 \times 10^{+5}/T) \rightarrow \text{BTU/lbmol(cal/gmol)}$$

The complete list of input parameters and operating conditions provided for the ReaCat Program is given in Kunii and Levenspiel (1969).

## Results

An $SO_2$ conversion of 59.74% is obtained (catalyst type: LP-120) at the exit point of the reactor and the outlet temperature is (1014 °F) 545.55 °C. If LP-110 catalyst is used, 45.99% conversion is obtained with an exit temperature of (950 °F) 510 °C. It can be seen that conversion is higher for LP-120, hence $SO_2$ emission will be less. Keeping the catalyst type constant and varying the inlet flow rate shows that decreasing the flow rate increases the conversion thus reducing $SO_2$ emission. Since this is an exothermic reaction, conversion decreases at higher temperatures. The process uses intermediate coolers to lower the temperature, which gives a better conversion and reduces $SO_2$ emission.

## Example 2, catalytic oxidation of ethanol in waste water

Organic pollutants dissolved in liquid water are usually removed by the biological oxidation process. However, some pollutants with aromatic structure decompose slowly under this process. Liquid-phase oxidation of organic pollutants in water with a solid catalyst provides a method that may remove dissolved organic compounds. This is a typical case when three-phase reactors are applied since the process contains liquid (aqueous

**Table 9.** Correlation used for the two-phase reactors

| | |
|---|---|
| Gas–liquid continuous stirred tank reactor | |
| 1. Maximum gas flow rate ($Q_{Gmax}$) | Charpentier (1981) |
| 2. Bubble diameter ($d_b$) | Van Dierendonck (1970) |
| 3. Gas holdup ($\epsilon_G$) | Van Dierendonck (1970) |
| 4. Liquid side mass transfer coefficient ($k_L$) | Van Dierendonck (1970) |
| Catalytic liquid fluidized-bed | |
| Mass transfer coefficient ($K_L$) | Chu et al. (1953) |
| Catalytic gas fluidized-bed | |
| 1. Voidage at minimum fluidization ($\epsilon_{mf}$) | Broadhurst and Becker (1975) |
| 2. Velocity at minimum fluidization ($U_{mf}$) | Kunii and Levenspiel (1969) |
| 3. Bubble diameter ($D_B$) | Horio and Nonaka (1987) |
| 4. Mass transfer coefficients ($K_{BC}$ and $K_{CE}$) | Kunii and Levenspiel (1969) |
| 5. Coefficient for axial dispersion ($D_{GA}$) | Kunii and Levenspiel (1969) |
| Catalytic gas fixed-bed | |
| 1. Coefficient for axial-dispersion | Kunii and Levenspiel (1969) |

**Table 10.** Calculation of catalytic effectiveness factor

| | |
|---|---|
| Catalytic effectiveness factor | $\eta = \frac{1}{\phi}\left(\coth 3\phi - \frac{1}{3\phi}\right)$ where $\phi$ is the Thiele modulus |
| First order reaction rate | |
| Spherical pellet | $\phi = \frac{R}{3}\sqrt{kSa\rho_P/De}$ |
| Cylindrical pellet | $\phi = \frac{R}{2}\sqrt{kSa\rho_P/De}$ |
| Slap pellet | $\phi = L\sqrt{kSa\rho_P/De}$ |
| General non-linear reaction rate | $\phi = \frac{R}{3}\rho p(-r(CS))\{\int_0^{C_{Sk}} 2Dek(-r(CS))dCSk\}^{-0.5}$ |
| where | |
| $k$ | Limiting reactant index |
| $D_{ek}$ | Effective diffusivity for the limiting reactant |
| $C_{Sk}$ | Limiting reactant concentration at catalyst surface |
| $(-r(C_s))$ | Intrinsic reaction rate as non-linear function of surface concentration |
| $R$ | Catalyst pellet radius |
| $\rho_P$ | Catalyst density |
| Limiting reactant is found by the following criterion | $D_{eB}C_{SB} > 10\nu D_{eA}C_{SA}$ |
| $\nu$ | Stoichiometry of B when stoichiometry of A=1 |
| $D_e$ | Effective diffusivity |
| $C_s$ | Surface concentration |

organic), gas (oxygen), and solid (catalyst). The objective of this analysis is to compare the ethanol conversion profiles for the different types of the three-phase reactors.

A typical catalyst used in this reaction is $Pd–Al_2O_3$ at 30 °C. The reaction has been shown to be first order with respect to oxygen and zero order with respect to ethanol. The reaction stoichiometry is represented as:

$A_g + B_l \rightarrow$ products

where

A Oxygen
B Ethanol
g Gas phase
l Liquid phase

The rate constant, $k$, is 0.0177 $cm^3/g$ s. Table 12 lists other parameters and operating conditions needed to run the ReaCat package. Since fixed-beds and suspended-beds have different characteristics regarding the catalyst load and catalyst particles diameter, different sizes of catalyst particles and catalyst loads were used in fixed-beds and suspended-beds. However, all other parameters and operating conditions are essentially the same in this comparison. Table 12 shows the different catalyst and reactor characteristics as used in the study.

## Design models and solution algorithms

A dispersion model is used to describe the liquid-phase component material balances in the following reactors: trickle-bed, bubble fixed-bed, bubble slurry, and three-phase fluidized. The gas phase was assumed to move in plug flow. Table 2 shows the component balance for the catalyst, gas, and liquid phase for the above reactors. Table 3 lists the component material balances in the well-agitated slurry reactor (CSTR slurry).

The catalytic effectiveness factor was calculated according to equations presented in Table 10. The gas–liquid and liquid–solid mass transfer coefficients were found using the correlations presented in Table 9. Values calculated for the mass transfer coefficients and catalytic effectiveness factors are given in Table 13.



## Results and discussions

The conversion profiles for the fixed-bed (trickle and bubble fixed-bed) and the suspended-bed (slurry and fluidized) reactor groups were compared separately because of the difference in catalyst load and particle size. However the catalyst load and particle size are the same within each group.

Figure 7 shows the ethanol conversion profiles in the trickle-bed and the bubble fixed-bed. The slight conversion increase in the bubble fixed-bed over the trickle-bed (about 4% at length=500 cm) is probably due to higher values of bubble fixed-bed mass transfer coefficients. The catalytic effectiveness factor for both of the fixed-bed reactors was found to be 0.13, while dispersion coefficients were negligible for both of these reactors in comparison with those for suspended-beds (Table 13).

Figure 8 shows a comparison of the ethanol conversion profiles in suspended-bed reactors. Similar catalyst loading and particle diameter were used in the three types of

**Table 11.** ReaCat, test cases

Catalytic gas fluidized-bed
Multiple reaction system for the production of phthalic anhydride from naphthalene (Kunii and Levenspiel)

| Literature | ReaCat (1) Plug flow | ReaCat (2) Plug flow | ReaCat Plug flow | Dispersion |
|---|---|---|---|---|
| Conversion | 97% | 94.93% | 85.49% | 81.26% |

(1) Experimental bubble diameter values has been used by the program
(2) The correlation of Horio and Nonaka (1984) has been used to find the bubble diameter

Continuous gas–liquid stirred tank reactor
Liquid phase oxidation of *o*-xylene into *o*-methylbenzoic acid by means of air (Froment and Bischoff 1979)

| | Literature | ReaCat |
|---|---|---|
| Conversion | 83.39% | 83.95% |

Trickle-bed
Liquid-phase oxidation of formic acid in the presence of CuO.ZnO catalyst (Baldi et al. 1974; Goto and Smith 1975)

| | Experimental | ReaCat (plug flow) | ReaCat (dispersion) |
|---|---|---|---|
| Conversion | 88.5% | 91.0% | 89.8% |

Continuous catalytic gas–liquid slurry stirred tank reactor
Hydrogenation of aniline to cyclohexylamine (supported nickel catalyst) (Govindarao and Murthy 1975; Ramachandran and Chaudhari 1983)

| | Literature | ReaCat |
|---|---|---|
| Reactor volume (46% conversion of Aniline) | 98 l | 99 l |

Semi-batch catalytic gas–liquid slurry stirred tank reactor
Butynediol synthesis by the reaction of gaseous acetylene with aqueous formaldehyde in the presence of copper acetylide catalysts(Kale et al. 1981)

| | Experimental | ReaCat (1) | ReaCat (2) |
|---|---|---|---|
| Conversion | 62% | 61.0% | 68.5% |

(1) Adsorption at catalyst surface is taking into account by the program
(2) No adsorption effects

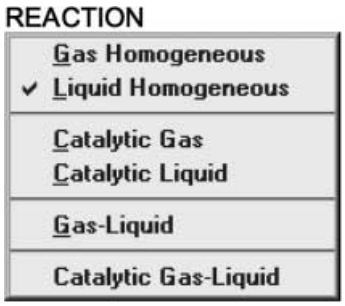




**Fig. 2.** Reaction phase menu

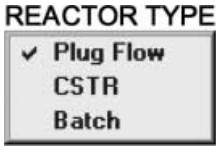


**Fig. 3.** Reactor type menu

suspended-beds. The catalytic effectiveness factor in suspended-beds was found to be much higher than that for fixed-beds (0.799 compared with 0.13 in fixed-beds) due to fine catalyst particles. The conversion profiles for the three-phase fluidized-bed and bubble slurry reactor had values that were very similar. The conversion in the three-phase fluidized-bed was higher by 9% than that in the bubble slurry reactor at length 500 cm. However, the conversion profile for the CSTR slurry reactor was much higher than in other suspended-beds. The conversion of ethanol in CSTR slurry was 52% higher than in the bubble slurry-bed and 37% higher than in the three-phase fluidized-bed at length 500 cm. The high conversion in the CSTR slurry reactor can be explained by the much higher mass transfer coefficients due to the mechanical agitation as seen in Table 13. The CSTR slurry reactor gave the best ethanol conversion among the suspended-beds, while the bubble fixed-bed gave the best conversion for the fixed-beds.

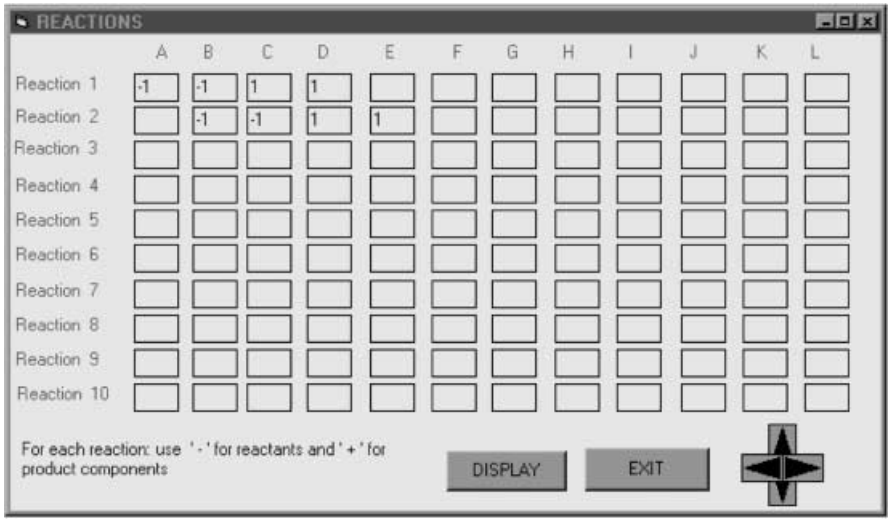


**Fig. 4.** Reaction stoichiometry input screen

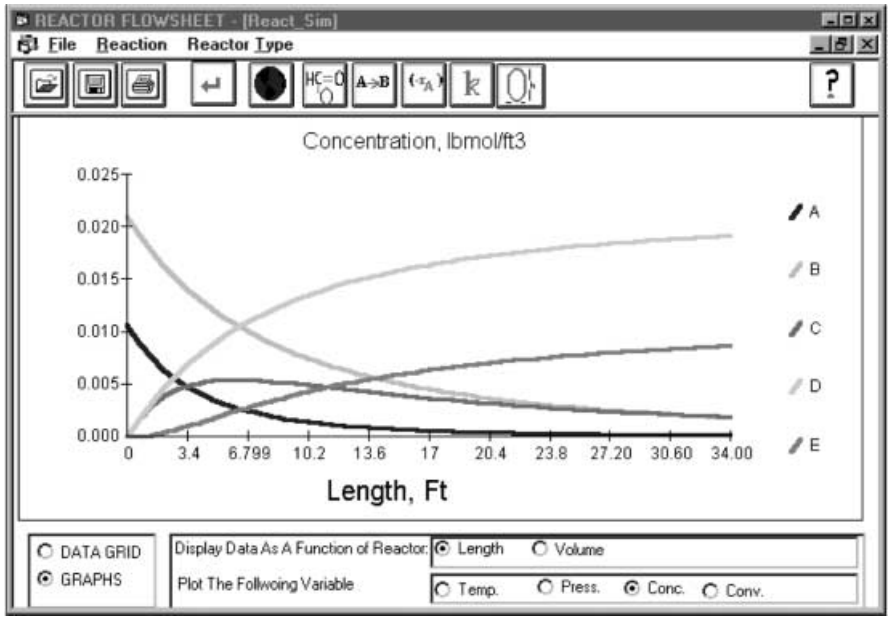


**Fig. 5.** An illustration of the graphical output of ReaCat program

**Table 12.** Parameters and operation conditions for the oxidation of ethanol

| Parameter or operating condition | |
|---|---|
| Catalyst particle diameter (cm) | Fixed-beds (trickle-bed and bubble fixed-bed)=0.5<br>Suspended-beds (slurry and fluidized-beds)=0.05 |
| Catalyst load (g/cm$^3$) | Fixed-beds=1.04<br>Suspended-beds=0.1 |
| Reactor diameter (cm) | 20 |
| Gas flow rate (cm$^3$/s) | 3140.0 |
| Liquid flow rate (cm$^3$/s) | 62.8 |
| Ethanol concentration in liquid-phase at inlet (mol/cm$^3$) | $4\times10^{-4}$ |
| Oxygen concentration at saturation (mol/cm$^3$) | $4.2\times10^{-6}$ |
| Molecular diffusivity (cm$^2$/s) | $4.7\times10^{-5}$ |
| Effective diffusivity (cm$^2$/s) | $4.16\times10^{-5}$ |
| Catalyst density (g/cm$^3$) | 1.2 |



**Table 13.** Mass transfer coefficients and catalytic effectiveness factor

| Reactor | Catalytic effectiveness factor | G–L mass transfer coefficient (1/s) | Liquid phase dispersion coefficient (cm$^2$/s) | L–S mass transfer coefficient (1/s) |
|---|---|---|---|---|
| Trickle-bed | 0.13 | 0.02 | 0.3266 | 0.0276 |
| Bubble fixed-bed | 0.13 | 0.144 | 0.9977 | 0.0408 |
| CSTR slurry | 0.799 | 1.05–1.45 | – | 1.14 |
| Bubble slurry | 0.799 | 0.02677 | 43.4 | 0.0952 |
| Three-phase fluidized-bed | 0.799 | 0.252 | 47.9 | 0.1 |

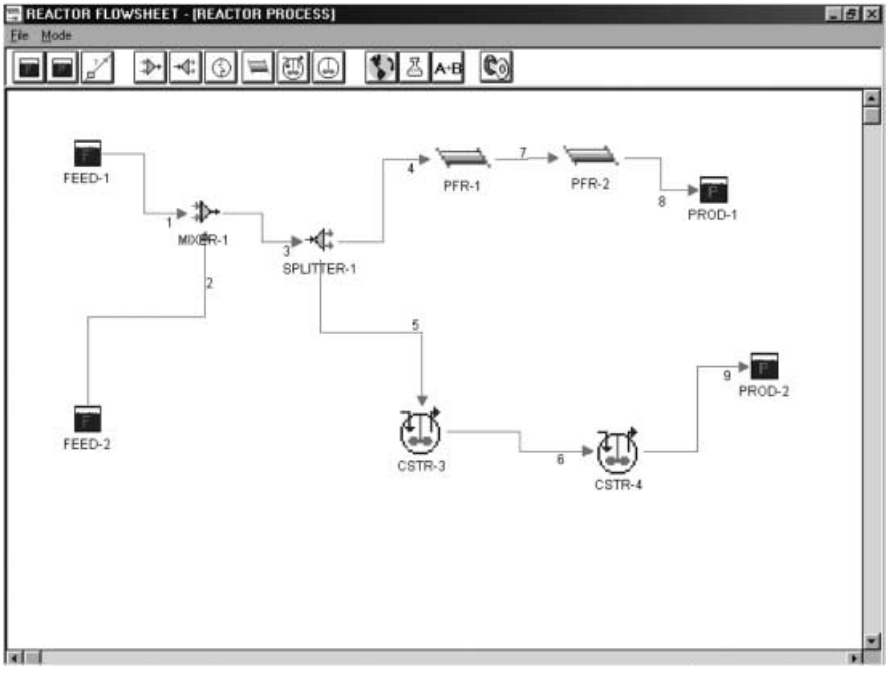


**Fig. 6.** Reactor flow-sheeting

This illustration of the use of the simulation package for these calculations demonstrates the significant capability to handle a very complex set of equations in a very effective and time saving manner. Other examples where simulation results were compared against experimental data have also been illustrated (Saleh 1994).

## Conclusion

A multi-phase catalytic reactor simulator has been developed. The simulation package has models to design the following reactor types: plug flow, CSTR, batch, catalytic fixed-bed, catalytic fluidized-bed, gas–liquid stirred tank, trickle-bed, three-phase fixed bubble-bed, bubble slurry column, CSTR slurry, three-phase fluidized-bed. Power-law reaction rates or the Langmuir–Hinshelwood models are included. It is equipped with correlation to estimate the external mass transfer effects (gas–liquid and liquid–solid) and dispersion coefficients. Estimation of the catalytic effectiveness factor to account for the intra-particle resistance is also included. Isothermal and non-isothermal/non-adiabatic conditions with multi-reaction systems with up to 30 reactions and 36 components are permitted.

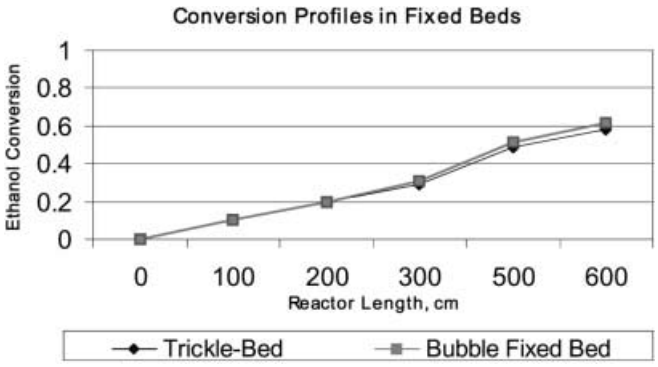




**Fig. 7.** Conversion of ethanol in three-phase fixed-beds

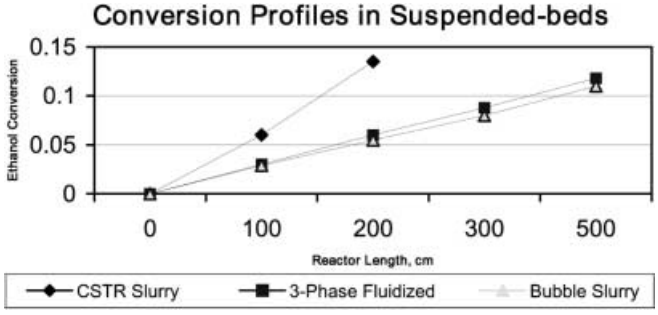


**Fig. 8.** Conversion of ethanol in three-phase suspended-beds

Reactor hydrodynamics such as pressure drop, power consumption, catalyst-wetting factor, and flow regimes may also be predicted.

## References

**Achwal SK, Stepanek JB** (1976) Holdup profiles in packed beds. Chem Eng J 12:69–75

**Akita K, Yoshida F** (1974) Bubble size, interfacial area, and liquid-phase mass transfer coefficient in bubble column. Ind Eng Chem Process Des Dev 13:84–91

**Baldi G, Gonti R, Alaria E** (1974) Catalytic oxidation of formic acid in water: Interparticle diffusion in liquid-filled pores. Chem Eng Sci 33:21–25

**Bern L, Lidefelt JO, Schoon NH** (1976) Mass transfer and scale-up in fat hydrogenation. J Am Oil Chem Soc 463–466

**Broadhurst T, Becker H** (1975) Onset of fluidization and slugging in beds of uniform particles. Am Inst Chem Eng J 21:238–247

**Calderbank PH** (1958) Physical rate processes in industrial fermentation. Part I, The interfacial area in gas-liquid contacting with mechanical agitation. Trans Inst Chem Eng 36:443–446

**Charpentier JC** (1981) Mass transfer rates in gas–liquid absorbers and reactors. Adv Chem Eng 11:2–133

**Chu JC, Kalil J, Weteroth WA** (1953) Mass transfer in fluidized bed. Chem Eng Prog 49:141–149

**Dakshinamurthy P, Subrahmanyam CCV, Kameswar RP** (1974) Studies of gas–liquid mass transfer in gas–liquid fluidized beds. In: Angelino H et al (eds) Fluidization and its applications. Cepadues, Toulouse

**Deckwer WD, Burchhart R, Zool G** (1974) Mixing and mass transfer in tall bubble columns. Chem Eng Soc 29:2177–2188

**Dhanuka VR, Stepanek JB** (1980) Gas–liquid mass transfer in three-phase fluidized bed. In: Matson JR (ed) Fluidization. Plenum, New York

**Dharwadkar A, Sylvester ND** (1977) Liquid–solid mass transfer in trickle-bed reactors. Am Inst Chem Eng J 23:940–944

**El-Temtamy SA, El-Sharnoubi YO, El-Halwagi MM** (1979) Liquid dispersion in gas–liquid fluidized beds. Chem Eng J 18:151–172

**Ellman MJ, Midoux G, Wild A, Laurent A, Charpentier JC** (1988) A new, improved pressure drop correlation for trickle-bed reactors. Chem Eng Sci 43:2201–2206

**Ellman MJ, Midoux G, Wild A, Laurent A, Charpentier JC** (1990) A new, improved liquid holdup correlation for trickle-bed reactors. Chem Eng Sci 45:1677–1683

**Fair JR** (1967) Designing gas-sparged reactors. Chem Eng 74:67–72

**Froment GF, Bischoff KB** (1979) Chemical reactor analysis and design. Wiley, New York

**Fukushima S, Kusaka K** (1979) Gas–liquid mass transfer and hydrodynamic flow in packed column with cocurrent upward flow. J Chem Eng Jpn 12:706–713

**Goto S, Smith JM** (1975) Trickle-bed reactor performance. Part I. Holdup and mass transfer effects. Am Inst Chem Eng J 21:706–720

**Govindarao VMH, Murthy KYR** (1975) Liquid-phase hydrogenation of aniline in a trickle-bed reactor. J Appl Chem Biotechnol 25:169–181

**Harris JL, Norman JR** (1972) Ind Eng Chem Process Des Dev 11:564

**Hedge SC** (1999) Simulation for pollution prevention: gas liquid reactors and sulfuric acid alkylation process. MSE Thesis, Lamar University

**Hochman JM, Effron E** (1969) Two-phase concurrent down flow in packed beds. Ind Eng Chem Fundam 8:63

**Horio M, Nonaka A** (1987) A generalized bubble diameter correlation for gas-solid fluidized beds. Am Inst Chem Eng J 33:1865–871

**Kale SS, Chaudhari RV, Ramachandran PA** (1981) Butyendiol synthesis. A kinetic study. Ind Eng Chem Prod Res Dev 20:309–314

**Kim SD, Baker CGJ, Bergougnou MA** (1975) Phase holdup characteristics of three-phase fluidized beds. Can J Chem Eng 53:134–139

**Kobayashi T, Saito H** (1965) Solid–liquid mass transfer in bubble columns. Kagaku Koide 3:210

**Kunii D, Levenspiel O** (1969) Fluidization engineering. Wiley, New York

**Larkins RP, White RR, Jeffery DW** (1961) Two-phase concurrent flow in packed beds. Am Inst Chem Eng J 7:231–239

**Lee JC, Sherrard AJ, Buckley PS** (1974) Optimum particle size in three-phase fluidized-bed reactor. In: Angelino H et al (eds) Fluidization and its applications. Cepadues, Toulouse

**Luong HT, Volesky B** (1979) Mechanical power requirements of gas–liquid agitated systems. Am Inst Chem Eng J 25:893–895

**Mangartz KH, Pilhofer T** (1981) Interpretation of mass transfer measurements in bubble columns considering dispersion of both phases. Chem Eng Sci 36:1069–1077

**Maselker RA** (1970) Bubble columns. Br Chem Eng 15:1297–1366

**Michel BJ, Miller SA** (1962) Power requirement of gas–liquid agitated systems. Am Inst Chem Eng J 8:262–266

**Michell RW, Furzer IA** (1972) Mixing in trickle flow through packed beds. Chem Eng J 4:53–63

**Ostergaard K** (1974) Gas-liquid-particle operation in chemical reaction engineering. Adv Chem Eng 7:71–137

**Pike RW, Hopper JR, Saleh J, Yaws CL, Hertwig TA, Chen X, Telang K** (1998) An advanced process analysis system for pollution prevention. In: Proceedings of Third International Conference on Foundations of Computer Aided Process Operations, Snowbird, Utah, 5–10 July. A.I.Che Symposium Series, No 320, Vol 94, pp 421–427

**Ramachandran PA, Chaudhari RV** (1983) Three phase catalytic reactors. Gordon and Breach, London

**Reiss LP** (1967) Cocurrent gas–liquid contacting in packed columns. Ind Eng Chem Process Des Dev 6:486–499

**Saleh JM** (1994) Computer simulation of three-phase catalytic gas–liquid reactions. Doctoral Dissertation, Lamar University, Beaumont, Texas

**Sano Y, Yamaguchi N, Adachi T** (1974) Mass transfer coefficients for suspended particles in agitated vessels and bubble columns. J Chem Eng Jpn 7:255–261

**Sato Y, Hirose H, Takahashi F, Toda M** (1973) Pressure loss and liquid holdup in packed-bed reactor with cocurrent gas–liquid down flow. J Chem Eng Jpn 6:147–152

**Shah TY** (1979) Gas–liquid–solid reactor design. McGraw-Hill, New York

**Specchia V, Baldi G** (1979) Heat transfer in trickle-bed reactors. Chem Eng Commun 3:483–488

**Specchia V, Sicardi S, Gianetto A** (1978) Absorption in packed towers with cocurrent flow. Am Inst Chem Eng J 20:646–653

**Stiegel GJ, Shah YT** (1977) Backmixing and liquid holdup in gas–liquid cocurrent up flow packed columns. Ind Eng Chem Process Des Dev 16:37–43

**Tarhan MO** (1979) Catalytic reactor design. McGraw-Hill, New York

**Telang KS** (1996) Advanced process analysis system. MSE Thesis, Chemical Engineering Department, Louisiana State University

**Tsutsumi A, Kim YH, Togawa S, Yoshida K** (1987) Classification of three-phase reactors. Sadhana 10:247–259

**Turpin JL, Huntington RL** (1967) Prediction of pressure drop for two-phase, two-component cocurrent flow in packed beds. Am Inst Chem Eng J 13:1196–1202

**Van Dierendonck LL** (1970) Vergrotingsregels voor gasbelwassers. Ph.D. Thesis, Twente University, Netherlands

**Van Krevelen DW, Krekels JTC** (1948) Rate of dissolution of solid substances. Part I.: physical dissolution. Recl Trav Chim Pays-Bas 67:512

**Waghchoure S** (1999) Simulation of two-phase catalytic fluidized bed reactors for pollution prevention. MSE Thesis, Lamar University, Beaumont, Texas

**Yamashita F, Aeon H** (1975) Gas holdup in bubble columns. J Chem Eng Jpn 8:334

**Yung CN, Wong CW, Change CL** (1979) Gas holdup and aerated power consumption in mechanically stirred tanks. Can J Chem Eng 57:672–677